

Effects of aging on the smoke from a large forest fire

L.F. Radke^{a,*}, A.S. Hegg^a, P.V. Hobbs^a, J.E. Penner^b

^a *Department of Atmospheric Sciences, AK-40, University of Washington, Seattle, Wash., USA*

^b *Lawrence Livermore National Laboratory, Livermore, Calif., USA*

Accepted 4 November 1994

Abstract

A smoke plume from a large wildfire in Oregon was sampled over a period of three days as it traveled more than 1000 km above the Pacific Ocean.

With increasing distance from the source, the dilution-normalized concentrations of particles in the nucleation mode ($D < 0.2 \mu\text{m}$) in the plume decreased rapidly and the average sizes of the particles in the accumulation mode ($D = 0.2 - 2.0 \mu\text{m}$) and coarse-particle mode ($D = 2.0 - 5.4 \mu\text{m}$) increased. The dilution-normalized optical scattering coefficient due to the particles in the smoke also decreased with increasing distance from the fire. Changes in the size distribution of the particles in the plume with distance downwind (age) are compared with numerical modeling results of particle coagulation and plume dilution and are found to be in reasonable agreement.

These rare field measurements of particle removal and modification rates in a dense, long-lived, plume are needed to help assess the role of biomass smokes as they relate to climate change. In the light of these measurements, it appears that the effects of particle coagulation in dense, persistent smokes may have been underestimated in some climate change calculations (e.g., nuclear winter) resulting in an overestimate of the smoke's impact.

1. Introduction

Smokes produced by the burning of biomass play an important role in atmospheric chemistry and in the climate of the Earth (e.g., MacCracken et al., 1986; UCAR, 1986; Penner et al., 1991 and Radke et al., 1991), as well as affecting local and regional air pollution (e.g., Sandberg et al., 1978). Penner et al. (1994) estimated that the effects of aerosol from biomass burning on the global radiation budget is about -0.8 W m^{-2} (central value) with a total uncertainty factor of about 2.5. A major fraction of this uncertainty is contained in effective emission factors (i.e., what fraction of the smoke escapes the near source environment) and smoke lifetime. Smoke lifetime also enters pivotally into the

* Corresponding author. Corresponding address NCAR, P.O. Box 3000 Boulder, CO 80307.

extreme climate change case of the widespread and dense smokes that would be produced by a major nuclear war. For this extreme case it has been calculated that average temperatures in the continental interiors of the northern hemisphere during late spring and early summer could be decreased by 15 to 35°C during the first few weeks of dense smoke (Pittock et al., 1986). In addition, smokes could have further effects on climate through modifying the microstructures of clouds (Twomey and Warner, 1967; Eagan et al., 1974; Twomey et al., 1984; Radke, 1989; Penner et al., 1993, 1994).

Thus to properly consider the large-scale impacts of smokes, it is important to have information on the effects of aging in the atmosphere on the properties of smoke from large fires. Only a few field measurements are available on this subject and none at scales and concentrations that could be considered realistic with respect to the nuclear winter hypothesis.

In this paper, we describe the results of airborne measurements in the plume of smoke from a large (3.9×10^4 hectares) uncontrolled forest fire of mostly coniferous timber that burned for over a month during August and September 1987 in the vicinity of Grant's Pass, Oregon, USA. We will refer to this as the Silver fire. Robock (1988) showed that the heavy pall of smoke from this fire reduced maximum daily temperatures at a few locations in northwestern California by as much as 20°C on occasions.

Although the Silver fire was a relatively large wildfire, the dispersion of the smoke plume was exceptionally slow due to synoptic conditions and the fact that the plume moved out over the Pacific Ocean where the atmosphere was quite stable. The low dispersion rate maintained high particle concentrations in the plume over the period of our measurements (3 days) and allows us to consider the concentration dependent effects observed as indicative of what could occur in much larger fires with more rapid dilution. This situation is particularly relevant to the widespread, continental-scale, biomass fires observed in Brazil and the savanna regions of Africa.

We obtained measurements of trace gases, particle size distributions, emission factors and light-scattering coefficients in the plume of smoke from the Silver fire from 17–19 September 1987. During this time we flew a distance of ~ 1000 km along the length of the plume in a series of flights as it moved SSW over the Pacific Ocean. The measurements obtained are described in this paper together with comparisons with a numerical model for particle coagulation and plume dilution. Implications for climate modification by biomass smoke and the nuclear winter hypothesis are discussed.

2. Flight tracks

During the period of our measurements, stable meteorological conditions produced a prominent smoke plume from the Silver fire that extended over 1000 km to the SSW over the Pacific Ocean (Fig. 1).

Shown in Fig. 2 is the flight path of the research aircraft with respect to the plume. Airborne measurements in the region of the densest smoke above the fire, were made at ~ 1400 PST on 17 September. For the next 3.5 h on 17 September the aircraft was flown down the axis of the plume for ~ 450 km. At 1730 PDT the aircraft emerged from the smoke and flew toward San Francisco for an overnight stop.

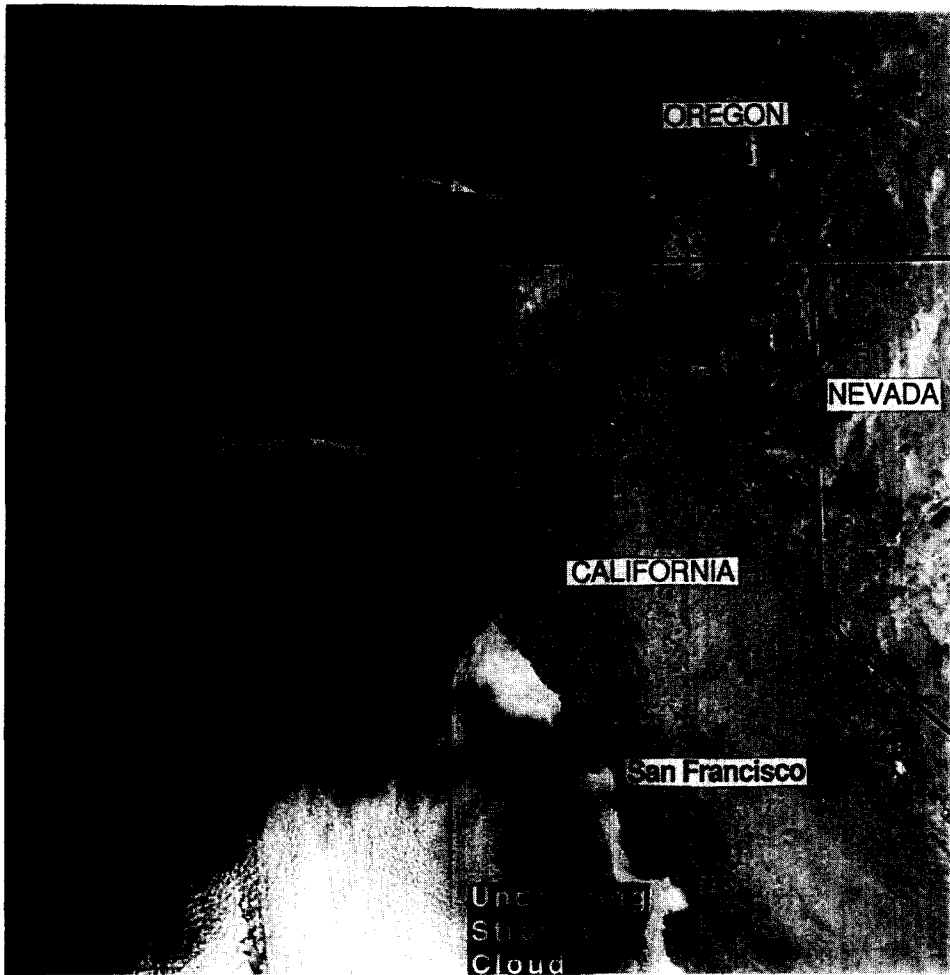


Fig. 1. Visible photograph taken at ~ 1600 UTC 17 September 1987 from the NOAA-9 AVHRR satellite showing the location of the Silver fire and the smoke plume it produced.

In San Francisco trajectory analysis was used to estimate where the portions of the plume sampled on 17 September might be found on the next day. Correctly calculated and flown this would have allowed us to make measurements of many “Lagrangian pairs” in the plume, separated in time by about 20 h. The advantage of such a sampling scenario is that one does not have to assume steady-state emissions from the fire when comparing Lagrangian pairs of measurements.

The aircraft departed San Francisco at 1040 PDT on 18 September and intercepted the plume at its predicted location at 1140 PDT. The aircraft was then flown down the axis of the plume for a distance of ~ 380 km, with measurements being made at several of the locations specified the previous evening for obtaining Lagrangian pairs with the measurements obtained on 17 September. During the entire flight on this day the smoke was situated above a shallow layer of marine stratus clouds. However, the cloud and smoke plume

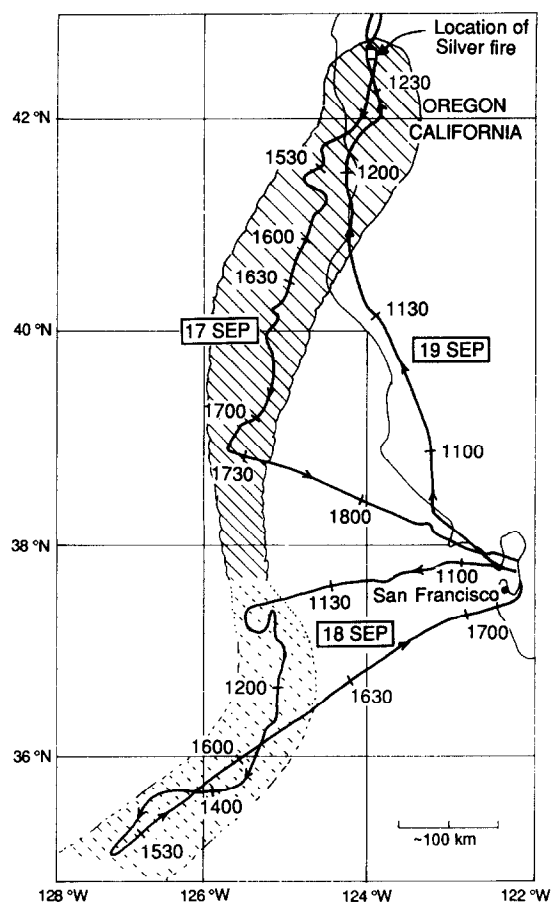


Fig. 2. Aircraft flight tracks (arrowed lines) in the plume of the Silver fire. The date and local time are shown at the various points on the aircraft track. The approximate horizontal extent of the visible plume from the Silver fire, derived from satellite imagery, is shown by the shaded region. The further extent of the plume, derived from the airborne measurements, is shown by the stippled area.

remained separate and the stable conditions prevented any direct interactions between them.

At ~1520 PDT the aircraft reversed course and flew back along the axis of the plume to land in Oakland at 1730 PDT.

The following day (19 September) the aircraft was flown northward up the California coast. The plume from the fire was located at 1145 PDT some 200 km south of the fire. Continuing north in the plume, the smoke above the fire was sampled in Oregon at ~1240 PDT.

Post-flight analysis, using additional meteorological data, including flight-level winds measured from the aircraft, showed that our attempt to obtain measurements as Lagrangian pairs was only partially successful. Only two sets of complete measurements (i.e. those including both aerosol and trace gas sampling) obtained on the latter half of the flight on 17 September were matched by Lagrangian pairs on the flight on 18 September. However,

many sets of partial measurements were Lagrangian pairs. We will see the conclusions drawn from the non-Lagrangian data where “steady state” emissions need to be assumed do not differ greatly from the Lagrangian data. Encouraged by this observation we have expanded the data set with the use of the steady-state assumption. However, other than the evidence that we will develop from the Lagrangian pairs, we have only modest additional evidence to offer concerning the temporal stability of the fire at its source. Wildfires are generally not steady-state for very long and they exhibit marked diurnal as well as shorter term variations. Fortunately for our experiment several factors worked toward stabilizing and homogenizing the source during the period of our observations.

- The Silver fire was not a single source. Within its boundaries hundreds of smaller fires burned in both isolation and along more organized lines.
- Wind speeds remained low, which limited rapid and highly variable spread of the fires.
- Foresters on the ground and in the air described the fires as “laid down” (i.e. very slowly moving with little visible flame from above) during this period with a great deal of smouldering combustion (D. Ward, pers. commun.).
- A smouldering fire characterization greatly reduces the variability in the CO/CO₂ ratio by reducing the fraction of emissions due to flaming combustion. This suggested our using the CO concentration as a conservative tracer for this experiment (Ward, 1990 and Laursen et al., 1992).

Nonetheless, the potential effects of time-varying emission on the non-Lagrangian portions of the data should be kept in mind.

3. Airborne instrumentation

The aircraft used for this study was the University of Washington’s Convair C-131A research aircraft. The aircraft was equipped with instrumentation for measuring the sizes and nature of aerosol and cloud particles, trace gas concentrations and various meteorological parameters. Major portions of the aerosol system have been described by Radke (1983) and Hegg et al. (1987). The aerosol instruments are routinely calibrated in house using a combination of techniques including a TSI Differential Mobility Particle Sizer, a Vibrating Orifice Aerosol Generator, a nebulizing system for monodisperse latex spheres and a dust generator to suspend various solid microspheres. Of equal importance to the calibration procedures is that the aerosol equipment is operated as a system with mature designs for inlets, sampling and sample distribution as well as adequate particle size range overlap with other instruments so that an important degree of “self-checking” is achieved. The primary instruments used in the present study are listed in Tables 1–3.

The aircraft made horizontal passes through the center of the smoke plume, where “grab” samples of air were collected for the determination of particle size distributions (averaged over ~0.5 km of flight path), carbonaceous trace gases and the total mass of particles (averaged over ~1 km of flight path). The center of the plume was considered to be located where the continuous measurements of particle number concentration and light scattering coefficient reached peak values while flying perpendicular to the plume axis.

Table 1

Principal instrumentation aboard the University of Washington's C-131A research aircraft used in this study

(a) Particle sizes and concentrations

Instrument	Equivalent particle diameter (μm)
Condensation nucleus counter*	> 0.005
Diffusion battery with condensation nucleus counter†	$\sim 0.01\text{--}0.1$
Electric aerosol analyzer†	$\sim 0.01\text{--}1.0$
Active scattering aerosol spectrometer†	$0.09\text{--}3$
Laser aerosol spectrometer†	$0.5\text{--}11$
Optical particle counter†	$2.6\text{--}48$
Forward-scattering spectrometer probe*	$3\text{--}45$

Table 2

(b) Trace gas chemistry

Gas	Technique	Detection Limit (ppbv)
SO_2^*	pulsed fluorescence	> 1
O_3^*	chemiluminescence (C_2H_4)	> 5
NO, NO_2^*	chemiluminescence (O_3)	> 1
$\text{CO}^†$	correlation IR spectrometer	> 100
$\text{CO}_2^†$	IR spectrometer	± 2 ppm
$\text{NH}_3^†$	impregnated filter	% variable
Whole air grab sample†	GC/mass spectrometer (post flight)	variable

Table 3

(c) Aerosol characteristics

Parameter	Instrument	Range
Light-scattering coefficient*	integrating nephelometer	$1 \times 10^{-6}\text{--}2.5 \times 10^{-3} \text{ m}^{-1}$
Light-extinction coefficient*	optical extinction cell	$5 \times 10^{-5}\text{--}10^{-2} \text{ m}^{-1}$
Particle mass†	quartz microbalance impactor	$< 2 \mu\text{m}$ diameter
		$\text{Cl}^- \pm 14\%$
Bulk aerosol chemistry†	Teflon filters, ion chromatography	$\text{SO} \pm 4\%$
(soluble anions concentration)		$\text{NO} \pm 11\%$
Particle morphology† and chemistry	impaction, electron microscopy	$> 0.2 \mu\text{m}$ diameter
Carbon soot§†	filtration, light absorption, pyrolysis	–

*Continuous measurements. †Grab sample measurements. §Analysis by Radiance Research and Sunset Laboratories.

4. Results

The ages of the smoke parcels that were sampled from the aircraft were estimated from 1-D trajectory analysis, using the northerly component of the winds measured from the aircraft as it traversed the length of the plume. The prevailing (fairly static) synoptic situation on 17 and 18 September justified the assumption of a steady northerly wind

component for the trajectory analysis. Also, the vertical stability combined with a temperature inversion that capped the plume at 1.2–1.5 km, which continuously confined the plume to a shallow, elevated, layer. These conditions allowed a determination of the age of the smoke parcels from a simple advection scheme, relating the age of a smoke parcel to the latitude at which it was sampled.

4.1. Particle emission factors

Particle emission factors (defined here as the mass of particles with diameters $< 3.5 \mu\text{m}$ diameter that are emitted per unit mass of wood burned) were determined using the carbon-balance method (Ward et al., 1982) as adapted to airborne measurements by Radke et al., 1989. The quantities that must be measured to apply this method are particle mass concentrations (derived here from the “grab” samples by weighing filters through which the smoke was passed), the mass concentrations of carbon dioxide, carbon monoxide, and total hydrocarbons (obtained from gas chromatography and mass spectrometer analysis (Westberg et al., 1974; Rasmussen et al., 1974), and the fractional mass of carbon in the particles [measured through elemental carbon analysis of sequenced pyrolysis of quartz filters exposed to the smoke (Johnson et al., 1981)].

The particle emission factor measured over the fire itself averaged 28 g kg^{-1} . This value is rather high compared to the average of 16 g kg^{-1} for ten large biomass fires reported by Radke et al., 1989. However, at the time we obtained measurements at the head of the fire (~ 1400 PST on 17 September) it consisted of widespread smouldering areas interspersed with a few much smaller regions that were burning intensely (D. Ward, pers. commun.). The measured particle emission factor is consistent with largely smouldering combustion, (Patterson and McMahon, 1984; Radke et al., 1991).

4.2. Particle size distributions

Shown in Fig. 3 are our measurements of the particle number and volume spectra for smoke parcels of four ages within the plume from the Silver fire. In order to make these particle spectra representative of the dimensions of the plume, the spectra shown for the head of the fire is the average of three samples and the 10, 25 and 44 h samples, where the plume was progressively wider, are the averages of 4, 4 and 5 samples, respectively, separated by 5–10 km. Factors that could have played a role in changing the particle size distribution with travel time (i.e. age) include dispersion of the plume, the coagulation and sedimentation of particles, and variations in the fire itself. We have found in our studies that while variations in fire size and intensity can introduce large changes in particle total number concentrations in the plume near a fire they typically produce only very modest changes in the geometric mean number diameter of particles in the accumulation mode. Thus the initial shapes of the particle size distributions in biomass fires are notable for their stability and similarity (Radke et al., 1989). Dilution decreases the number concentration of particles in the plume; the effects of this can be seen in the number concentrations of particles with diameters $> 1 \mu\text{m}$ (Fig. 3). The comparatively high particle concentrations measured after 25 h of aging (curve C in Fig. 3) are a notable exception to this trend and could be due to a brief variation in fire behavior. Thus, the counter trend anomalous

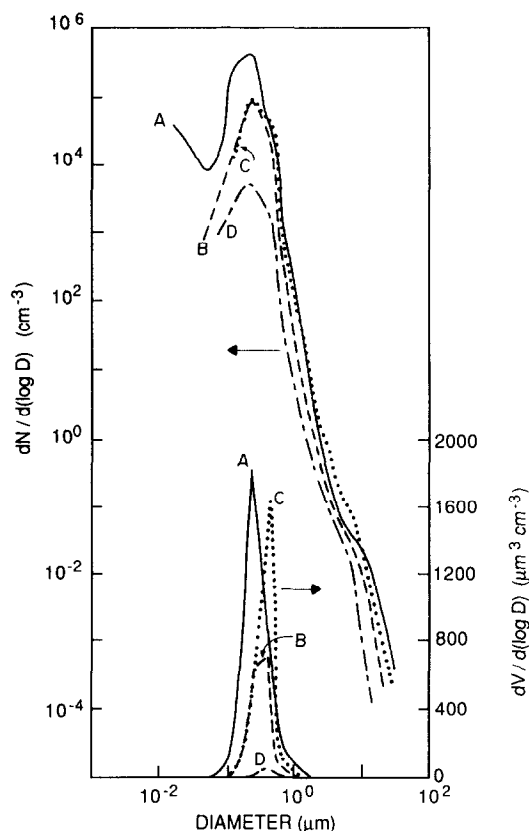


Fig. 3. Particle number and volume spectra measured at the head of the Silver fire (A), and at 10 h (B), 25 h (C) and 44 h (D) travel time of the smoke downwind of the fire.

distribution shown in curve C is this considered as probably concentration anomalous, but is included here for the sake of completeness.

In dense smokes, such as these, coagulation is likely to play an important role in changing the particle size spectra. This is apparent in the accumulation mode ($D = 0.2\text{--}2.0\ \mu\text{m}$) of the particle volume spectra (Fig. 3). For these particles, the particle diameter (D_m) at which the volume concentration reaches a maximum value increases steadily with the age of the smoke up to 25 h. However, D_m for the smoke at 44 h is nearly the same as the D_m at 25 h. This is consistent with the rate of particle coagulation in a plume decreasing sharply as the plume dilutes (e.g. Fuchs, 1964). This interpretation is borne out by the results shown in Fig. 4. Up to about 25 h, the geometric mean volume diameter (Fig. 4a) and geometric mean number diameter (Fig. 4b) of the particles in the accumulation mode increased with age for all samples. The rate of increase is positively correlated with the light-scattering coefficient due to dry particles, which is generally proportional to the mass concentration of particles in the accumulation mode (Waggoner et al., 1981).

To investigate the effects of particle coagulation and sedimentation on various properties of the plume we first corrected for dilution of the plume due to dispersion by assuming that



Fig. 4. (a) Geometric mean volume diameter and (b) geometric mean number diameter of particles in the accumulation mode ($0.2\text{--}2 \mu\text{m}$ diameter) as a function of the age of the smoke in the plume of the Silver fire. The measurements are differentiated by the value of the light-scattering coefficient due to dry particles (β_{sp}) as follows: Stars and dotted lines: $2 \times 10^{-4} \text{ m}^{-1} < \beta_{\text{sp}} < 5 \times 10^{-4} \text{ m}^{-1}$; triangles and dashed lines: $5 \times 10^{-4} \text{ m}^{-1} < \beta_{\text{sp}} < 10^{-3} \text{ m}^{-1}$; circles and solid lines: $\beta_{\text{sp}} > 10^{-3} \text{ m}^{-1}$.

carbon monoxide (CO) was a conserved constituent in the plume for the Lagrangian pairs and further assume that the CO source strength is a constant for the other samples. We will refer to concentrations of species in the plume that have been adjusted to eliminate the effects of dilution due to dispersion (by dividing by the concurrently measured above-ambient concentration of CO) as *dilution normalized*.

Shown in Figs. 5, 6 and 7 are the dilution normalized volume concentrations of particles in the nucleation, accumulation and coarse-particle modes, respectively, for the smoke in the Silver fire as a function of age. If dispersion were the only process causing the concen-

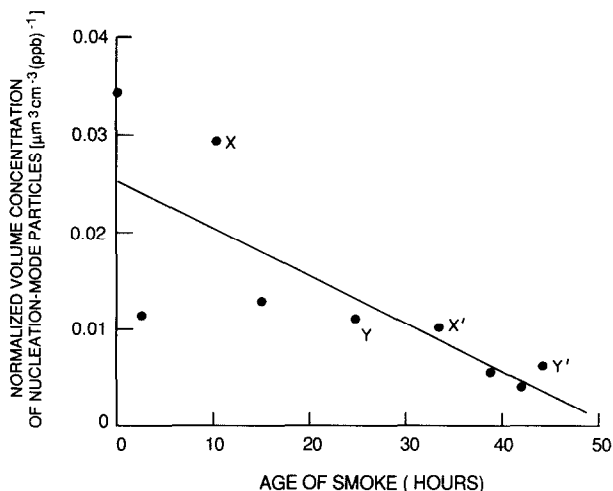


Fig. 5. Dilution-normalized volume concentrations of particles in the nucleation mode ($<0.2 \mu\text{m}$ diameter) as a function of the age of the smoke in the plume of the Silver fire (correlation coefficient $r = -0.77$). X – X' and Y – Y' indicate two Lagrangian pairs of measurements.

trations of the particles in the plume to decrease, the dilution-normalized concentrations would remain constant with age. In fact, these figures show that the dilution-normalized volume concentrations of particles in the nucleation and accumulation modes both decreased with age, but those in the coarse-particle mode increased with age. A qualitative interpre-

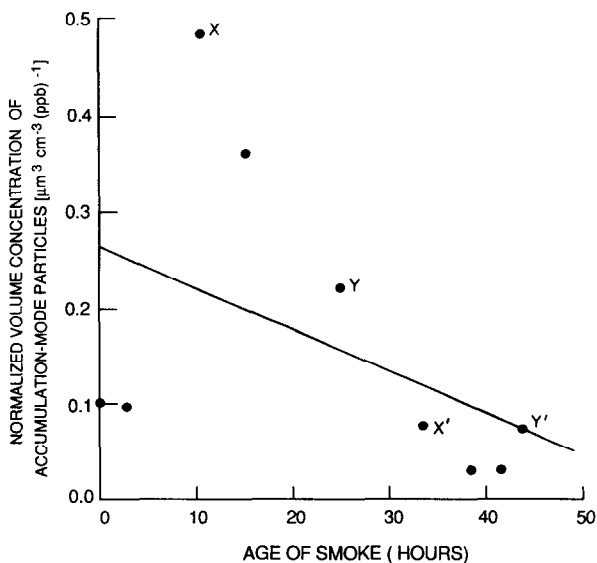


Fig. 6. As for Fig. 5 but for particles in the accumulation mode ($r = -0.47$).

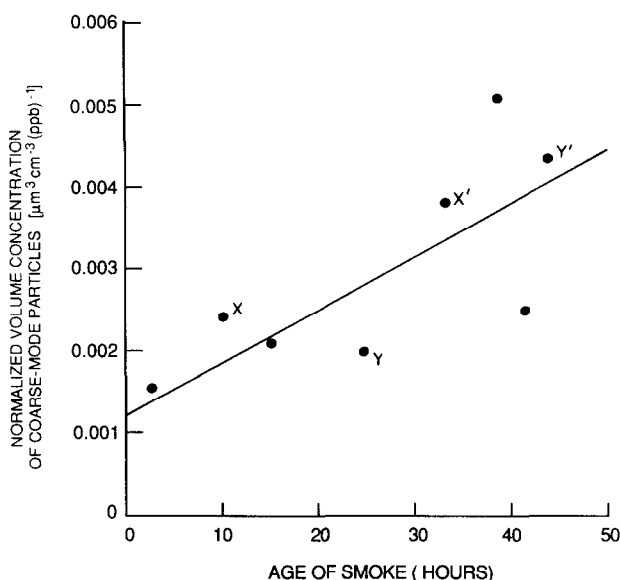


Fig. 7. As for Fig. 5 but for particles in the coarse particle mode ($r=0.81$).

tation of these results is as follows. The decrease with age in the dilution-normalized volume concentrations of the particles in the nucleation mode was due to their rapid coagulation with particles in the accumulation mode. The decrease with age in the dilution-normalized volume concentrations of particles in the accumulation mode was presumably due to their coagulation and transfer to the coarse particle mode, which therefore increased in concentration with time. Interestingly, coagulation theory for spherical particles does not predict such a significant transfer of accumulation mode particles into the coarse mode (see Section 5). The trend indicated in the dilution-normalized volume concentration of accumulation mode particles (Fig. 6) compared to that of coarse mode particles (Fig. 7), suggests not only that a significant fraction of the accumulation mode volume transferred to the coarse mode but that these particles were removed from the plume, possibly by sedimentation.

At first glance it appears unlikely that sedimentation can account for the large removal rates that were observed, since a *spherical* particle $2\text{ }\mu\text{m}$ in diameter only fall 10's of meters per day. However, $5\text{ }\mu\text{m}$ diameter particles fall more than 100 m per day, which is sufficient to remove a significant fraction of these particles from the rather shallow plume. Furthermore, the effective density of the smoke particles may rise at the same time as their drag decreased with time due to the coagulating particles becoming more spherical aggregates (Friedlander, 1977).

4.3. Changes in the optical properties of the smoke with age

The decrease in the dilution-normalized light scattering coefficient of the particles (β_{sp}), shown in Fig. 8 corresponds roughly to the observed decrease with age of the dilution-normalized volume concentration in the accumulation mode (Fig. 6). After 11 h of aging,

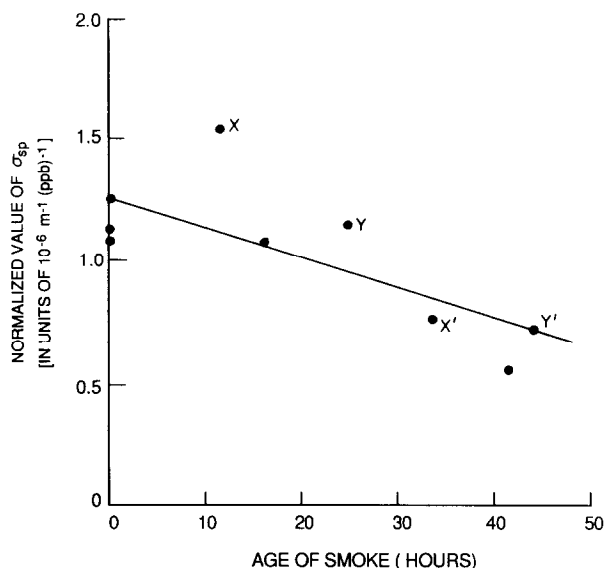


Fig. 8. As for Fig. 5 but for the light-scattering coefficient due to dry particles ($r = -0.78$).

coagulation apparently shifts the particle volume distribution to larger sizes, serving to decrease the dilution-normalized volume concentrations of particles in the accumulation mode was presumably due to their coagulation and transfer to the coarse particle mode, which therefore increased in concentration with time. change in the particle size distribution support this interpretation.

4.4. Satellite observations

The NOAA-9 AVHRR imagery was examined for the time period of these observations (P. Durkee et al., unpubl. manuscript). The ratio of channels 1 and 2 (0.63 and 0.86 μm center wavelengths) using appropriate corrections for geometry and the underlying surfaces (Durkee, 1984) is directly related to the shape of the aerosol size distributions. The satellite data was analyzed from near the coastline until the plume approached the northern boundary of the status deck west of San Francisco. Because the channel 1 radiance is more closely linked to the accumulation mode and channel 2 to the coarse mode aerosol, the relative rates of decrease of these channels is approximately linked to the relative roles of particle coagulation and sedimentation removal. Durkee et al. (in prep.) concludes from their analysis that from about 7 to 20 h downwind coagulation dominated the observed changes in plume optical properties. They further conclude that the observed change in the ratio of channel 1 and 2 is consistent with the flattening of the size distribution shown in Fig. 3 at 0, 25 and 44 h. Similar conclusions are drawn by Westphal and Toon, 1991.

4.5. Uncertainties

The observations described above represent measurements over an exceptional spatial scales and under circumstances which, while not unique, will only rarely permit replication.

The plan was to obtain many true “Lagrangian pairs” however, only two were obtained. These pairs have been supplemented with a reasonable, but arguable, use of CO as a conservative tracer. Thus, alternative interpretations of some of our observations are possible.

5. Comparisons with numerical modeling calculations

We have employed a numerical model to aid our analysis of the observed evolution of the particle size distributions in the smoke plume. The model, which has been described by Penner and Porch (1987), computes the effects on particle size distributions of dilution and Brownian coagulation by solving the equation

$$\frac{dn(r)}{dt} = \frac{1}{2} \int_0^r K(r', r-r') n(r') n(r-r') dr' - \int_0^\infty K(r, r') n(r') dr' - \frac{n(r)}{\tau_d}$$

where $n(r) = dn/dr$ is the number concentration of spherical particles with radii between r and $r+dr$, τ_d the dilution time constant, and $K(r, r')$, the coagulation kernel between particles of radius r and r' . The first and second terms in the equation represent the increase and decrease, respectively, in particle concentration due to coagulation. The model employs the formulation of Fuchs (1964) of $K(r, r')$ for spheres. The last term represents the reduction in particle concentration due to dilution of the plume, the formulation of which assumes that all sizes of particles dilute with ambient air at equal rates. As a test, the model has reproduced the time-dependent changes in the self-preserving size distribution described by Friedlander (1977) under a variety of initial conditions.

For the Lagrangian pair of measurements determined through our trajectory analysis (age 11 and 33 h) we calculated a value of 3.1×10^4 s for τ_d , with a standard deviation of 1.3×10^4 s. This dilution rate was computed from the change of integrated volume in the measured particle volume distributions for the pair (where the measured distributions are each the average of four individual samples). We calculated the standard deviation of τ_d using error analysis, taking into account statistical uncertainties in average wind speeds, sampling positions, and the particle volume concentrations in the smoke samples. This uncertainty was dominated by the variation in measured wind speeds used in the trajectory analysis.

To test whether dilution and Brownian coagulation can explain the observed changes in the size distributions in the Lagrangian pair of measurements, we have compared the output from the numerical model with the measurements at 11 and 33 h in Fig. 9. The measured distribution at 33 h generally falls within the range of uncertainty for the model output in the accumulation mode. This agreement is expected, since dilution is a significant factor in the evolution of the distributions; the dilution rate was derived from the change in particle volume, and the particle volume distribution is dominated by the accumulation mode. There are more nucleation mode particles in the measured distribution at age 33 h than in the model output; this could be attributable to the creation of new particles in the plume by gas-to-particle conversion. Also, there are more coarse mode particles in the measured distribution at 33 h than in the model output. This difference is within the uncertainty of the

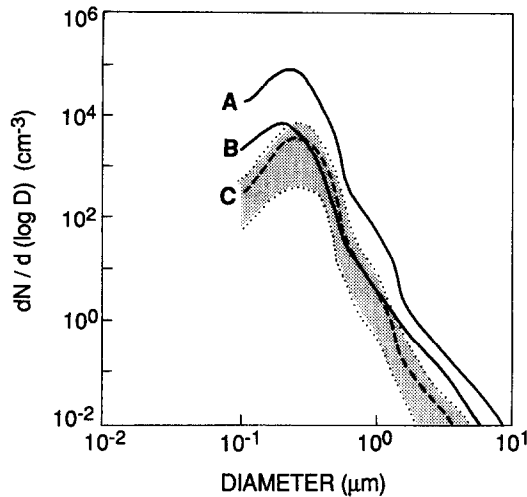


Fig. 9. Comparison of calculated and measured particle number distributions in the plume of smoke from the Silver fire. (A) Distribution measured after 11 h of aging. This distribution was used to initialize the model. (B) Measured distribution after 33 h of aging. (C) Model-derived distribution after 33 h of aging. The envelope shows the range of uncertainty in the calculated distribution due to uncertainties in the value of the derived dilution constant.

averaged distributions at large particle sizes, which is not shown. The absolute uncertainty in the measured number concentrations for a particle of radius $1\ \mu\text{m}$ is about a factor of two due to the steep slope of the distribution and the calibration uncertainty in size (the counting accuracy uncertainty is small as is the repeatability), and for a particle of radius $2.25\ \mu\text{m}$ the relative uncertainty is even larger. These models improved results and our experimental data suggest that some previous analyses of the effects of coagulation have underestimated the removal of accumulation mode particles in the cases of dense, long-lived plumes (Turco et al., 1983a, b; Crutzen et al., 1984; National Research Council, 1985).

6. Implications

The field measurements described in this paper show that particle size distributions in smoke change significantly as the smoke ages. The light-scattering coefficient (normalized to remove the effects of plume dilution) of the smoke also decreased significantly with the age of the smoke. We have shown that the principal features of the changes in particle size distribution with age can be explained by particle coagulation in the smoke and dilution of the plume. It also appears that the effects of smoke particle coagulation may have been underestimated in some calculations of the effects of smoke on the Earth's atmosphere and especially on global and regional climate.

These observations notably combine real smoke particles, at high number smoke densities (which persist for days) that are realistic for either the distributed fires found at continental scales above fire scarred tropical forest and grass lands and needed for climate calculations

or similarly in the nuclear winter hypothesis. Thus, while the experiment is also modestly flawed in execution and contains some uncertainties which are difficult to quantify, it has the virtue of an illustrated, real world example which contains the actual physics of the aerosol transport phenomena rather than a theoretical construct.

Our deductions of faster than expected aerosol removal (according to some theoretical models) by coagulation and sedimentation, as well as decreased light scattering efficiency with time, may also be used to address a puzzling satellite observation recently observed in Brazil. The biomass smokes of Brazil produce, seasonally, a nearly continental-scale pall of smoke that is detected by satellite sensors such as the NOAA AVHRR (Setzer and Pereira, 1991; Kaufman, 1987). During the fire season, the smoke accumulates in a vast anti-cyclonic pall, influenced by the tropical Atlantic and blocked by the Andian cordillera. Periodically these polluted air masses are forced off the continent and out over the South Atlantic Ocean. Surprisingly, AVHRR data show that only a very small fraction of the expected smoke escapes the continent in this fashion (L. Stowe, personal communication). Where does the rest of the smoke go? The “loss” mechanisms by coagulation described here may be a part of the answer. The same mechanism(s) may act to reduce global distribution and climate effects of aerosols.

The same observed effects that act to modestly ameliorate the impact of biomass smokes on regional and global climate should also act to reduce the effects of the wide-spread smokes that would be associated with nuclear war, the so called nuclear winter hypothesis. In the National Research Council (1985) review of the nuclear winter hypothesis, attention was focused on a smoke with a rather stable particle size distribution; the number mode diameter (equivalent to our number mode diameter for the accumulation mode, since the NRC report did not consider the possibility of a significant lifetime for particles in the nucleation mode) increased from the size of the primary particles to $\sim 0.2 \mu\text{m}$ near the source with no change thereafter. It was stated that only under unusual circumstances would coagulation be more important and the accumulation mode size increase beyond $\sim 0.2 \mu\text{m}$. Turco et al. (1983a, b) noted that there might be circumstances where the coagulation of particles could increase the accumulation number mode diameter by $\sim 65\%$ in one week (which would be in reasonable accord with our results), but that more reasonable assumptions with rapid smoke dispersion would reduce the effects of coagulation to a negligible effect shortly after emission. Similarly, Crutzen et al. (1984) calculated an increase in number mode diameter of less than a factor of two after one month of aging. As a result, in many of the discussions of the nuclear winter hypothesis, particle coagulation in the smoke has been considered as having only a secondary or negligible effect on particle removal rates and the optical properties of the particles [i.e. not necessary to be included in the model, although some modeling results (Penner and Porch, 1987) had suggested a more important role for coagulation]. The field measurements described in this paper clearly indicate that the NRC scenario underestimates the effects of particle coagulation. As we have seen, the particles in the dense portions of the smoke plume from the Silver fire coagulated rather rapidly, resulting in both rapid increases in the number mode diameter of particles in the accumulation mode and apparently significant losses by sedimentation. Presumably, in the dense smokes produced by a nuclear war, coagulation would also move a significant mass of the smoke into the coarse particle mode where sedimentation would more readily remove the particles from the atmosphere.

Coagulation also provides a mechanism for moving smoke particles out of the precipitation scavenging minimum ($\sim 0.1\text{--}1\text{ }\mu\text{m}$ diameter) to sizes large enough to be scavenged more efficiently by precipitation and for the particles to become more efficient cloud condensation nuclei and cloud scavenged with increased efficiency (Dana and Hales, 1977; Radke et al., 1980; Rogers et al., 1991). Moreover, the rapid coagulation of smokes from a variety of sources (e.g., oil supplies and biomass) would allow the aggregated smoke to tend toward the cloud nucleating properties of the most active smoke. This would permit smoke particles, which initially might be ineffective as cloud condensation nuclei, to be removed through nucleation scavenging in clouds. Finally, the coagulation of particles in smokes could produce a marked decrease in their light scattering efficiencies, leading to a reduction in the optical depth of the smoke, regardless of removal mechanisms.

We conclude that at the high particle concentrations found in the dense smokes from large fires, the coagulation of particles can play an important role in modifying particle size distributions, reducing optical extinction and speeding the removal of particles. All of these effects should cause the impact of the smokes to be mitigated more rapidly than would otherwise be the case.

Acknowledgements

We are also grateful to Drs. Philip Durkee, Douglas Westfall and Darold Ward for their help in the field study. Cray-2 computer resources were provided by the Lawrence Livermore National Laboratory. This research was supported by the Defense Nuclear Agency, through funds made available under NRL Contract N00014-86-C-2246, the Sandia National Laboratory under Document 57-0343, and the USDA Forest Service under Agreement PSW-87-0020CA. Work at LLNL was performed under the auspices of the U.S. Department of Energy under Contract no. W-7405-Eng-48. Portions of this work were carried out at the National Center for Atmospheric Research. The National Center for Atmospheric Research is operated by the University Corporation for Atmospheric Research under sponsorship of the National Science Foundation.

References

- Crutzen, P.J., Galbally, I.E. and Brühl, C., 1984. Atmospheric effects from post-nuclear fires. *Clim. Change*, 6: 323–364.
- Dana, M.T. and Hales, J.M., 1977. Washout coefficients for polydisperse aerosols. In: R.G. Semonin and R.W. Beadle (Editors), *Precipitation Scavenging*. Technical Information Center Energy Research and Development Administration, Springfield, Virginia, Conf. Rep. 741003, pp. 247–257.
- Durkee, P.A., 1984. *The Relationship between Marine Aerosol Particles and Satellite-detected Radiance*. Ph.D. Thesis, Colorado State Univ., Ft. Collins, CO, 124 pp.
- Durkee, P.A., Devries, P.J., Radke, L.F. and Westfall, D., in prep. Satellite and aircraft observations of smoke particle characteristics.
- Eagan, R.C., Hobbs, P.V. and Radke, L.F., 1974. Measurement of cloud condensation nuclei and cloud droplet distributions in the vicinity of forest fires. *J. Appl. Meteorol.*, 13: 553–557.
- Friedlander, S.K., 1977. *Smoke, Dust and Haze*. Wiley, New York, 317 pp.
- Fuchs, N.A., 1964. *The Mechanics of Aerosols*. Pergamon Press, New York, 408 pp.

- Hegg, D.A., Radke, L.F., Hobbs, P.V., Brock, C.A. and Riggan, P.J., 1987. Nitrogen and sulfur emissions from the burning of forest products near large urban areas. *J. Geophys. Res.*, 92: 14,701–14,709.
- Johnson, R.L., Shah, J.J., Cary, R.A. and Huntziker, J.J., 1981. An automated thermal-optical method for the analysis of carbonaceous aerosol. In: E.S. Marcias and P.K. Hopke (Editors), *Atmospheric Aerosol: Source/Air Quality Measurements*. Symposium Series, 167. Am. Chem. Soc. Washington, D.C., pp. 223–233.
- Kaufman, Y.J., 1987. Satellite sensing of aerosol absorption. *J. Geophys. Res.*, 92: 4307–4317.
- Laursen, K., Hobbs, V., Radke, F. and Rasmussen, R.A., 1992. Some trace gas emissions from North American biomass fires with an assessment of regional and global fluxes from biomass burning. *J. Geophys. Res.*, 97: 20,687–20,701.
- MacCracken, M.C., Cess, R.D. and Potter, G.R., 1986. Climatic effects of anthropogenic arctic aerosols: an illustration of climatic feedback mechanisms with one- and two-dimensional climate models. *J. Geophys. Res.*, 91: 14,445–14,450.
- National Research Council Committee on Atmospheric Effects of Nuclear Explosions, *The Effects on the Atmosphere of a Major Nuclear Exchange*. National Academy Press, Washington, D.C.
- Patterson, E.M. and McMahon, C.K., 1984. Absorption characteristics of forest fire and particulate matter. *Atmos. Environ.*, 18: 2541–2551.
- Penner, J.E. and Porch, W.M., 1987. Coagulation in smoke plumes after a nuclear war. *Atmos. Environ.*, 21: 957–969.
- Penner, J.E., Ghan, S.J. and Walton, J.J., 1991. The role of biomass burning in the budget and cycle of carbonaceous soot aerosols and their climate impact. In: J.S. Levine (Editor), *Global Biomass Burning*. The MIT Press, Cambridge, Massachusetts, pp. 387–393.
- Penner, J.E., Charlson, R.J., Hales, J.M., Laulainen, N., Leifer, R., Wovakov, T., Ogren, J., Radke, L.F., Schwartz, S.E. and Travis, L., 1993. Quantifying and minimizing uncertainty of climate forcing by anthropogenic aerosols. NTIS, NTIS DOE/NBB-092T UC-402, 53 pp.
- Penner, J.E., Charlson, R.J., Hales, J.M., Laulainen, N., Leifer, R., Novakov, T., Ogren, J., Radke, L.F., Schwartz, E.E. and Travis, L., 1994. Quantifying and minimizing uncertainty of climate forcing by anthropogenic aerosols. *Bull. Am. Meteorol. Soc.*, 75: 375–400.
- Pittcock, A.B., Ackerman, T.P., Crutzen, P.J., MacCracken, M.C., Shapiro, C.S. and Turco, R.P., 1986. *Environmental Consequences of Nuclear War, Vol. 1: Physical and Atmospheric Effects*. Wiley, New York, 359 pp.
- Radke, L.F., 1983. Preliminary measurements of the size distributions of cloud interstitial aerosol. In: H.R. Pruppacher, R.G. Semonin and W.G.N. Slinn (Editors), *Precipitation Scavenging, Dry Deposition and Resuspension*. Elsevier, New York, pp. 71–78.
- Radke, L.F., 1989. Airborne observations of cloud microphysics modified by anthropogenic forcing. In: *Proc. Symp. Role of Clouds in Atmospheric Chemistry and Global Climate, January 30–February 3, 1989, Anaheim, California*. Am. Meteorol. Soc., pp. 310–318.
- Radke, L.F., Hegg, D.A., Hobbs, P.V., Nance, J.D., Lyons, J.H., Laursen, K.K., Weiss, E., Riggan, P.J. and Ward, D.E., 1991. Particulate and trace gas emissions from large biomass fires in North America. In: J.S. Levine (Editor), *Global Biomass Burning*. The MIT Press, Cambridge, Massachusetts, pp. 387–393.
- Radke, L.F., Hobbs, P.V. and Eltgroth, M.W., 1980. The scavenging of aerosol particles by precipitation. *J. Appl. Meteorol.*, 19: 715–722.
- Radke, L.F., Hegg, D.A., Lyons, J.H., Brock, C.A. and Hobbs, P.V., 1989. Airborne measurements on smokes from biomass burning. In: P.V. Hobbs and M.P. McCormick (Editors), *Aerosols and Climate*. A. Deepak Publishing, Hampton, Virginia, pp. 411–422.
- Rasmussen, R.A., Westberg, H.H. and Holdren, M.W., 1974. Need for standard referee GC methods in atmospheric hydrocarbon analyses. *J. Chromatogr. Sci.*, 12: 80–84.
- Robock, A., 1988. Enhancement of surface cooling due to forest fire smoke. *Science*, 242: 911–913.
- Rogers, C.F., Hudson, J.G., Hallett, J. and Penner, J.E., 1991. Cloud droplet nucleation by crude oil smoke and coagulated crude oil/wood smoke particles. *Atmos. Environ.*, 25A: 2571–1580.
- Sandberg, D.V., Pierovich, J.M., Fox, D.G. and Ross, E.W., 1978. Effects of fire on air, USDA Forest Service General Tech. Rep. WO-9, U.S. Government Printing Office, Washington, D.C.
- Setzer, A., Pereira, M. and Pereira, A., 1990. AVHRR Estimates of Biomass Burning during BASE-A. Paper presented at the Chapman Conference on Global Biomass Burning: Atmospheric, Climatic, and Biospheric Implications, Williamsburg, Va., 19–23 March.
- Turco, R.P., Toon, O.B., Ackerman, T.P., Pollack, J.B. and Sagan, C., 1983. Nuclear winter: global consequences of multiple nuclear explosions. *Science*, 222: 1283–1293.

- Turco, R.P., Toon, O.B., Ackerman, T.P., Pollack, J.B. and Sagan, C., 1983b. Global atmospheric consequences of Nuclear War. Interim report. R and D Associates, Marina del Ray, California, 144 pp.
- Twomey, S.A., Pipegrass, M. and Wolfe, T.L., 1984. An assessment of the impact of pollution on global cloud albedo, *Tellus*, 36B: 356–366.
- Twomey, S.A. and Warner, J., 1967. Comparisons of measurements of cloud droplets and cloud nuclei. *J. Atmos. Sci.*, 24: 702–703.
- University Corporation for Atmospheric Research (UCAR), 1986. Global Tropospheric Chemistry: Plans for the U.S. Research Effort, Office for Interdisciplinary Earth Studies. Boulder, Colorado, 110 pp.
- Waggoner, A.P., Weiss, R.E., Ahlquist, N.C., Covert, D.S., Will, S. and Charlson, R.J., 1981. Optical characteristics of atmospheric aerosols. *Atmos. Environ.*, 15: 1891–1909.
- Ward, D.E., 1990. Factors influencing the emissions of gases and particulate matter from biomass burning. In: J.G. Goldammer (Editor), *Fire in the Tropical Biota: Ecosystem Processes and Global Challenges*. Springer, New York, pp. 418–436.
- Ward, D.E., Sandberg, D.V., Ottman, R.D., Anderson, J.A., Hofner, G.G. and Fitzimmons, C.K., 1982. Measurements of smoke from two prescribed fires in the Pacific Northwest. In: *Proc. 75th Annu. Meet. Air Pollution Control Association*. Air Pollution Control Association, Pittsburgh, Pennsylvania, Pap., 82-8.40.
- Westberg, H.H., Rasmussen, R.A. and Holdren, M.W., 1974. Gas chromatographic analyses of ambient air for light hydrocarbons using a chemically bonded stationary phase. *Anal. Chem.*, 46: 1852–1854.
- Westphal, D.L. and Toon, O.B., 1991. Simulations of microphysical, radiative, and dynamical processes in a continental-scale forest fire smoke plume. *J. Geophys. Res.*, 96: 22,379–22,400.